Catalysis Science & Technology

Hydrolysis of Amides to Carboxylic Acids Catalyzed by Nb_2O_5

Journal:	*Catalysis Science & Technology*
Manuscript ID	CY-ART-11-2020-002230.R1
Article Type:	Paper
Date Submitted by the Author:	25-Dec-2020
Complete List of Authors:	Siddiki, S.; Hokkaido University, Institute for Catalysis, N-21,W-10 Rashed, Md. Nurnobi; Hokkaido University Touchy, Abeda; Hokkaido University, Catalysis Research Center Jamil, Md.; Hokkaido University, Catalysis Jing, Yuan; Hokkaido University Toyao, Takashi; Hokkaido university, Institute for Catalysis Maeno, Zen; Hokkaido University, Institute for Catalysis Shimizu, Ken-ichi; Hokkaido University, Catalysis Research Center

Hydrolysis of Amides to Carboxylic Acids Catalyzed by Nb_2O_5

S. M. A. Hakim Siddiki,[†]* Md. Nurnobi Rashed,[†] Abeda Sultana Touchy,[†] Md. A. R. Jamil, [†] Yuan Jing,[†] Takashi Toyao,[†,‡] Zen Maeno,[†] Ken-ichi Shimizu*[†,‡]

[†] Institute for Catalysis, Hokkaido University, N-21, W-10, Sapporo 001-0021, Japan

[‡] Elements Strategy Initiative for Catalysts and Batteries, Kyoto University, Katsura, Kyoto 615-8520, Japan.

*Corresponding author

S. M. A. Hakim Siddiki, Ken-ichi Shimizu

E-mail: hakim@cat.hokudai.ac.jp, kshimizu@cat.hokudai.ac.jp

Abstract

Hydrolysis of amides to carboxylic acids is an industrially important reaction but is challenging due to the difficulty of cleaving the resonance stabilized amidic C–N bond. Twenty-three heterogeneous and homogenous catalysts were examined in the hydrolysis of acetamide. Results showed that Nb_2O_5 was the most effective heterogeneous catalyst with the greatest yield of acetic acid. A series of Nb_2O_5 catalysts calcined at various temperatures were characterized and tested in the hydrolysis of acetamide to determine the effects of crystal phase and surface properties of Nb_2O_5 on catalytic performance. The high catalytic performance observed was attributed mainly to the facile activation of the carbonyl bond by Lewis acid sites that function even in the presence of basic inhibitors (NH_3 and H_2O). The catalytic studies showed the synthetic advantages of the present method, such as simple operation, catalyst recyclability, additive free, solvent free, and wide substrate scope (> 40 examples; up to 95% isolated yield).

KEYWORDS: Nb_2O_5 Catalyst, Amide hydrolysis, Carboxylic acid, C=O bond activation, Lewis acid.

Introduction

Amides are a ubiquitous functional moiety in organic compounds and are a fundamental structural unit in proteins, peptides, enzymes, polymers, and drugs. Amides also are involved in most of the biological functions of plants.[1] Functional conversion of amides is important in organic syntheses,[2–9] but is challenging due to the necessity of cleaving the resonance stabilized amidic C–N bond (Fig. 1).[10–13]

Hydrolysis involves a water nucleophile that produces oxygen-containing compounds from salts, esters, amides, adenosine triphosphate (ATP), cellulose, metal aqua ions, and others.[14–16] Hydrolysis of amides, including peptides, proteins, and amino acid amides, to the corresponding acids is an important reaction in industrial and biochemical process.[17] Extensive effort has been employed toward the hydrolysis of amidic C–N bond of peptides in proteins to examine the protein structure/function/folding processes and target-oriented protein-cleaving drug design using efficient and selective artificial proteases.[18–21] These artificial proteases and the conventional enzyme-mediated hydrolysis of peptide have limited substrate scope, require post-translational modification, experience interference in the structural mapping of peptides, and require strict pH and temperature control. Metal-substituted polyoxometalates (MSPs) (also called artificial proteases) include highly Lewis acidic metal ions such as Zr^{IV} and Ce^{IV}, which are remarkably effective homogeneous catalysts in peptide hydrolysis.[18–22] However, these methods have the disadvantages of limited catalyst reusability and catalyst/product separation difficulties. Chemical hydrolysis methods that have advantages over enzymatic methods have been developed by exploiting metal

complexes or metal ions as Lewis-acid catalysts, which facilitate cleavage of peptides containing unnatural amino acids.[23] Parac-Vogt and co-workers demonstrated the first heterogeneous catalytic method of peptide bond hydrolysis using immobilized Zr^{IV} in MOF-808.[24] All Lewis-acid-mediated hydrolytic processes were accelerated significantly by the formation of hydrolytically active species from an amine nitrogen, amide oxygen, and Lewis-acidic metal ion, followed by polarization of the peptide bond that allowed access for nucleophilic attack by water.

Few studies have been done on the catalytic hydrolysis of free amides other than those focused on peptides. However, conventional strong acid-base-mediated hydrolysis of amides has had the problem of producing a large amount of unwanted by-products.[25–27] Enzymatic hydrolysis of amides is a classic method for synthesizing the corresponding carboxylic acids.[15] However this approach is limited by substrate scope and selectivity, and requires strict pH and temperature control. Stoichiometric use of homogeneous metal ion catalysts along with Cu, Ni, Co, and Zn was reported to promote the hydrolysis of selective amino acid amides,[28] and a dinuclear Ni complex was used to catalyze the hydrolysis of urea and piconilamide.[29] Microwave-irradiated indirect hydrolysis of free amides to the corresponding carboxylic acids and potassium carboxylate was demonstrated using silica-assisted phthalic anhydride[30] and potassium fluoride doped alumina,[31] respectively. However, these methods were conducted under non-aqueous conditions and/or with *in situ* water generation. Direct hydrolysis of amides in water is desirable because it can be environmentally friendly ("green") and has the potential for large-scale syntheses. Therefore, the development of a hydrolytic synthesis of amides to carboxylic acids using reusable solid acid catalysts would be a significant contribution.

In general, catalysts with Lewis acid and/or Brønsted acid sites play a key role in activating oxygen-containing functional groups.[8,9,32–35] However, difficulties arise when a base or a Lewis acid inhibitor suppress Lewis acidity through chelation. Classic Lewis acid catalysts, along with $AlCl_3$ and BF_3, undergo decomposition in water.[36–38] Metal triflates, such as $Sc(OTf)_3$ and $Yb(OTf)_3$, are excellent water-tolerant homogenous Lewis acid catalysts for activation of carbonyl compounds.[39–43] Niobium oxides/niobic acid catalysts also are established base- and water-tolerant Lewis acid catalysts and show high activity/selectivity in acid-catalyzed reactions. [32,44–58] Recent reports on the transformation of carboxylic acid derivatives demonstrated that the surface of Nb_2O_5 could catalyze nucleophilic substitution reactions of acids, esters, anhydrides, and amides in the presence of Lewis acid inhibitors, including water, alcohols, and amines.[32,59–63] This property of niobium oxide indicates that coordinatively superficial Nb^{5+} cation acts as an active Lewis acid site to activate C=O moieties in carboxylic acid derivatives while simultaneously not engaging in competitive adsorption of other base molecules.[64,65]

The present study describes heterogeneous Nb_2O_5 catalysts with different structures (amorphous and crystalline phases)[66–68] for direct hydrolysis of amides to carboxylic acids with water. The Lewis acid nature of Nb_2O_5 that can activate the C=O bond of the amide moiety promotes efficient

progression of the reaction along with the basicity originating from the lattice oxygens. As a result, Nb_2O_5 calcined at a mid-range temperature of 500 °C, with both acid and base sites, was found to be the best catalyst for amide C–N bond-breaking hydrolysis.

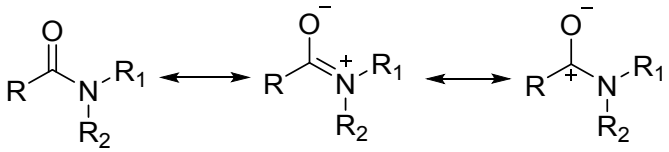

Rotation barrier C-N bond = 15-20 kcal/mol
Resonance energy = 19-26 kcal/mol
Bond length C-N bond = 1.33 Å

Fig. 1 Stability of amidic resonance structures.

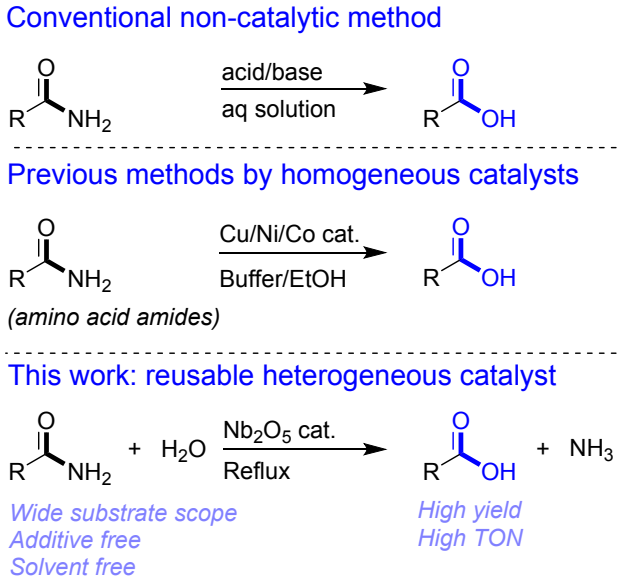

Scheme 1 Hydrolysis of amides to carboxylic acids.

Results and discussion

Catalyst screening and reaction condition optimization

To optimize reaction conditions and find the most effective catalysts, a comprehensive survey of reaction parameters was obtained for hydrolysis of acetamide (**1a**) into acetic acid (**2a**). A series of catalysts, including acidic, basic, heterogeneous, and homogeneous types, underwent screening in the model hydrolysis reaction of acetamide **1a** (1 mmol) and water (5 mmol) without any solvent at reflux under an N_2 atmosphere for 20 h. The yield of acetic acid **2a** based on acetamide **1a** using different catalysts is shown in Table 1. The reaction did not produce any acetic acid **2a** without a catalyst (Table 1, entry 1). Various metal oxides (treated and untreated) were used in this model reaction (entries 2–13), with Nb_2O_5 providing the maximum yield of acetic acid in 20 h (97%, entry 2). The reflux condition, which eliminates the NH_3 formed in the reaction system is key to obtaining high yields, otherwise strong thermodynamic limitations associated with reverse reactions between the acid formed and NH_3 hinder progression of C–N bond cleavage (temperature-dependent equilibrium conversion is given in Fig. S1). A moderate to low yield (4–53%; entries 4-7) of acetic acid was obtained by introducing acidic oxides, including ZrO_2, TiO_2, SnO_2, and SiO_2. Amphoteric oxides such as ZnO, CeO_2, and Al_2O_3 also provided low to moderate yields of acetic acid (6–45%; entries 8-10). The basic oxides, CaO, MgO and La_2O_3 (entries 11-13), which had low activity in this hydrolysis reaction, provided **2a** in 3–17% yield. The Brønsted acid catalysts, Hβ-20 and HMFI-20 (entries 14-15), were relatively inactive in this amide hydrolysis reaction. Commercially available solid catalysts, including montmorillonite K10 clay (entry 16) and Nafion-SiO_2 composite (entry 17), resulted in lower yields of **2a** compared to that using Nb_2O_5 catalyst. Typical water-tolerant homogeneous Lewis acid $Sc(OTf)_3$ (entry 18) afforded **2a** in 47% yield. The reaction also was tested with typical metal salts, including ammonium niobite(V) oxalate hydrate ($C_4H_4NNbO_9 \cdot xH_2O$), cerium nitrate [$Ce(NO_3)_4$], and zirconium sulphate tetrahydrate [$Zr(SO_4)_2.4H_2O$] (entries 19-21), which provided **2a** in 45%, 31%, and 25% yield, respectively. In addition, homogenous Brønsted acid catalysts (PTSA, H_2SO_4; entries 22, 23) were less active in this hydrolysis reaction. Note that conventional homogeneous catalysts generate a lower yield of acetic acid under the same catalyst weight conditions. Results of these extensive catalyst screening reactions revealed that Nb_2O_5 was the most effective catalyst for hydrolysis of acetamide **1a** to acetic acid **2a**.

Understanding the relation between the properties of heterogeneous catalysts and their function is challenging but is needed to understand the underlying phenomena and to develop improved catalysts. We have recently reported that catalyst reactivity for another C–N bond-breaking reaction, *i.e.*, alcoholysis of amides, is governed mainly by basicity of the metal oxide catalyst because nucleophilic attack of the lattice oxygen atom on the carbonyl carbon atom of the amide is the rate-determining step for the catalytic process.[9,35] The lower the O_{1s} binding energy of metal oxides determined by X-ray photoelectron spectroscopy (XPS) analysis, the more rapid the reaction rates of

the C–N bond-breaking reaction due to the greater basicity of the metal oxide surface.[69] In addition, an *in situ* IR study was conducted by adsorbing *N,N*-dimethylacetamide on various metal oxide catalysts, because the position of the C=O stretching bands (ν_{CO}) of *N,N*-dimethylacetamide is a measure of Lewis acidic nature, especially for activation processes of C=O moieties of carboxylic acid derivatives including amides.[32,64] Results demonstrated that CeO_2 was the best catalyst for alcoholysis of amides because CeO_2 has both acid and base sites to activate the amide.

In the present study, carboxylic acid formation rate per surface area of the catalysts via hydrolysis of acetamide was plotted as a function of IR band positions of the C=O stretching mode of *N,N*-dimethylacetamide adsorbed and O_{1s} binding energy of the metal oxide catalyst, as shown in Fig. 2. *N,N*-Dimethylacetamide was used because its C=O moiety has behavior similar to that of the acetamide used for the standard reaction.[9,70] Note that the values used for the x-axis were taken from previous reports[9,71] and carboxylic acid formation rates (y-axis) were obtained from reactions with yields less than 30%. The Nb_2O_5 and ZrO_2, both of which exhibit a strong red shift of the position of the C=O stretching bands, had high initial reaction rates, with ZrO_2 found to be the best when the activity was normalized by surface area. In contrast, catalysts such as SiO_2 and MgO, which do not have strong Lewis acid sites to activate the carbonyl oxygen of amides, had low initial reaction rates. Moreover, a weak correlation was found between reaction rate and O_{1s}-binding energies, as shown in Fig. 2B, which suggests that surface basicity plays a role in promoting amide hydrolysis in a manner similar to that of C–N bond cleavage alcoholysis of amides. These results demonstrate that both acidic and basic properties are important for efficient progression of the hydrolysis reaction, with Lewis acidic character especially important for activating the C=O moiety. Thus, Nb_2O_5 and ZrO_2 possessed excellent catalytic performance, and, Nb_2O_5, with its greater surface area, had the greatest activity. The initial normalized reaction rate of formation of carboxylic acid as a function of the O_{1s} binding energies shows that the Nb_2O_5 catalyst with moderated level of basicity is the second-best in activity and the best in the full-time reaction, TOF, TON and reusability with base and water tolerance.

Using Nb_2O_5, reaction conditions were optimized for this model hydrolysis reaction and are shown in Table 2. In the hydrolysis of 1.0 mmol acetamide (**1a**), 50 mg Nb_2O_5 catalyst were required to afford 97% of product acetic acid (**2a**) using 10 mmol of water (entries 1-5). Subsequently, examination of the effect of water amount revealed that the hydrolysis reactions proceeded even when reducing the amount of water; 97% yield of acetic acid was achieved using 5 mmol of water. A further decrease in the amount of water (4,3,2 mmol) suppressed the hydrolysis reaction. Based on these results, the optimized reaction conditions were: Nb_2O_5 catalyst (50 mg), acetamide **1a** (1 mmol), water (5 mmol), under reflux for 20 h.

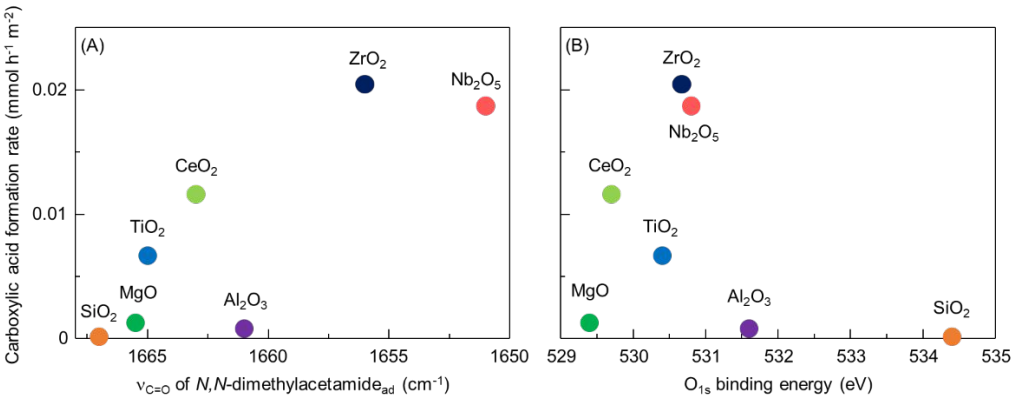

Fig. 2 (A) Correlation between initial reaction rates of carboxylic acid formation from hydrolysis of acetamide and IR band positions of the C=O stretching mode of *N,N*-dimethylacetamide adsorbed onto the oxides, measured at 40 °C[9] and (B) XPS O_{1s} binding energies.[71]

Table 1. Catalyst screening for hydrolysis of acetamide to acetic acid.

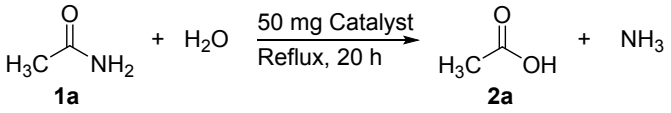

1a **2a**

1 mmol 5 mmol

Entry	Catalyst (surface areas m^2/g)	Conv.(%)	Yield (%)[a]
1	none	2	0
2	Nb_2O_5 (82)	100	97
3	Na^+- Nb_2O_5	80	78
4	ZrO_2 (44)	54	53
5	TiO_2 (45)	17	15
6	SnO_2	9	8
7	SiO_2 (268)	6	4
8	ZnO	9	7
9	CeO_2 (69)	47	45
10	Al_2O_3 (74)	7	6
11	CaO	5	4
12	MgO (24)	5	3
13	La_2O_3	19	17
14	Hβ-20	2	0
15	HMFI-20	2	0
16	Montmorillonite K10	11	10
17	Nafion-SiO_2	15	14
18	$Sc(OTf)_3$	49	47
19	$C_4H_4NNbO_9.nH_2O$	47	45
20	$Ce(NO_3)_4$	33	31
21	$Zr(SO_4).4H_2O$	26	25
22	*p*-toluenesulfonic acid (PTSA)	7	5
23	H_2SO_4	4	3

[a] GC yield.

Table 2. Optimization of reaction conditions for hydrolysis of acetamide to acetic acid.

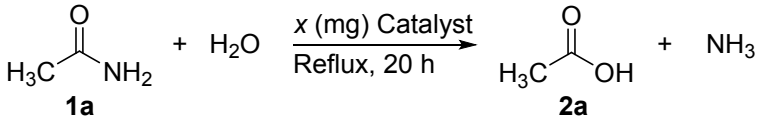

1a 1 mmol *y* (mmol) **2a**

Entry	(*x* mg) Nb_2O_5	(*y* mmol) water	Yield (%)[a]
1	20	10	52
2	30	10	70
3	40	10	83
4	50	10	96
5	60	10	97
6	50	5	97
7	50	4	88
8	50	3	68
9	50	2	47

[a] GC yield.

Structure-activity relation and mechanism of Nb_2O_5 catalysts

After choosing the most favorable catalyst and reaction conditions, the relation between structure and catalytic activity was investigated for various Nb_2O_5 catalysts toward hydrolysis. Fig. S2 shows X-ray diffraction (XRD) patterns of Nb_2O_5 catalysts containing various peaks that were detected upon an increase in calcination temperature. Results showed several crystal forms of Nb_2O_5 polymorphs were obtained. The Nb_2O_5 polymorphs could be subdivided into several phases such as pseudo-hexagonal (TT), orthorhombic (T), tetragonal (M), monoclinic (B), and monoclinic (H), based on calcination temperature.[72] At a lower calcination temperature (200 °C), the catalyst was completely amorphous. A mixture of TT and T phases formed at 500 °C calcination. Only the crystalline T phase was observed at a calcination temperature of 700 °C.[66] The TT and T phases were structurally very similar; the only difference was the presence of a legitimate defect of oxygen atoms in the TT phase that made it less crystalline than the T-phase. That caused a broadening of XRD peaks at 2θ = 29° and 2θ = 37° (Cu Kα radiation) in the TT phase. In contrast, splitting of the same peaks occurred in the T phase due to formation of (180) and (181) planes.[32] Thus, T-Nb_2O_5 was stabilized by closely spaced Nb atoms having separate and equivalent sites, whereas TT-Nb_2O_5 was stabilized by impurities such as OH^-, Cl^-, or oxygen vacancies.[73] In addition, high temperature calcination (1000 °C) produced XRD patterns that contain diffuse and sharp peaks. These results resemble those from formation of Nb_2O_5 M and B phases, respectively. However, the H phase crystallizes at 1150 °C calcination.[74] Therefore, the TT phase is the least stable phase, while the H phase is the most thermodynamically stable.[32] Overall, temperature-dependent crystal forms of Nb_2O_5 catalysts were identified.

The N_2 adsorption experiments were performed to determine the specific surface areas of different Nb_2O_5 polymorphs. The N_2 adsorption isotherms are shown in Fig. S3. The Brunauer-Emmett-Teller (BET) method was used to obtain the specific surface areas. Results showed that the surface area of niobium oxides decreased as the calcination temperature increased (Fig. 3A). The acid properties of Nb_2O_5 catalysts also were investigated by pyridine adsorption IR experiments (Fig. S4). The IR absorption bands at 1445 cm^{-1} and 1540 cm^{-1} were assigned to adsorption of pyridine on superficial Nb^{5+} cations as Lewis acidic sites and H^+ cations from Brønsted acid sites of Nb_2O_5 catalysts, respectively.[59] Subsequently, the numbers of Lewis and Brønsted acid sites on different Nb_2O_5 catalysts were calculated from the area intensities of the bands at 1445 cm^{-1} and 1540 cm^{-1}. The average integrated molar extinction coefficients 1.73 cm μmol^{-1} and 1.23 cm μmol^{-1} were used to obtain the number of Lewis and Brønsted acid sites, respectively.[75] Increasing the calcination temperature caused a gradual decrease in the amount of acid sites (Fig. 3B). After calcination at temperatures at 1000 °C or higher, acid sites on niobium oxides were almost eliminated.

To understand how crystallinity changes the acidity that affects the hydrolysis reaction, the initial reaction rate and turnover frequency (TOF), which was defined as the initial reaction rate per surface Lewis acid site, were determined at different calcination temperatures (Fig. 3C and 3D). Note

that the initial reaction rates were obtained with a shorter reaction time (2 h) in the hydrolysis of acetamide. As calcination temperature increased, surface area and acid sites decreased. And the initial rate of hydrolysis decreased accordingly. On the other hand, a volcano-shaped trend was observed for TOF. Nb_2O_5 prepared by 500 °C calcination was found to show the greatest initial hydrolysis rates per surface area, indicating a Nb_2O_5 catalyst in the TT or T phase with a moderate number of Lewis acid sites is effective for the hydrolysis reaction.

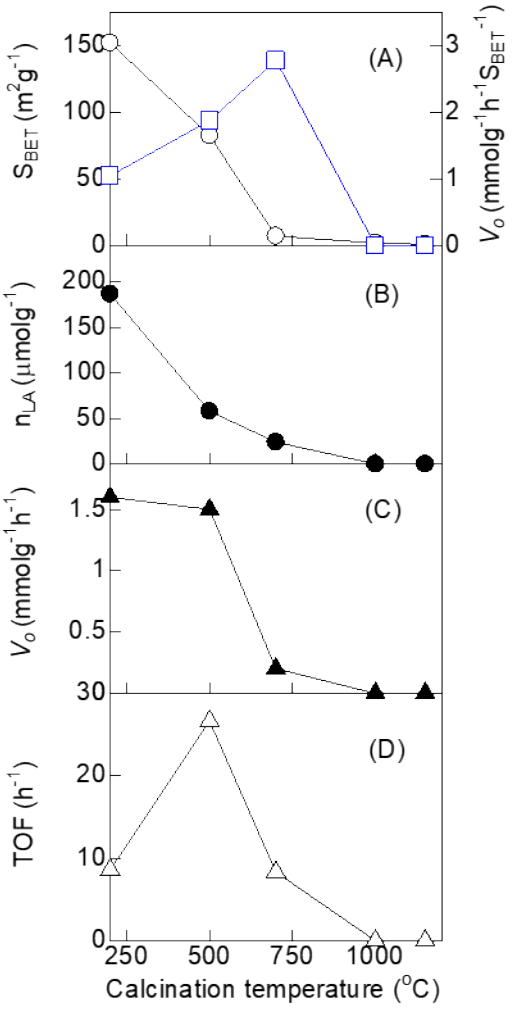

Fig. 3 (A) BET surface area and initial rate of hydrolysis of acetamide per surface area (B) number of Lewis acid sites of different Nb_2O_5 catalysts calcined at different temperatures determined by N_2 adsorption and pyridine adsorption IR experiments, respectively. (C) Initial rate for hydrolysis of acetamide, and (D) TOF, defined as initial reaction rate per surface Lewis acid site using Nb_2O_5 catalysts calcined at different temperatures. Reaction conditions: acetamide 1 mmol, water 5 mmol, catalyst 50 mg, reflux for 2 h.

In situ IR spectroscopy was used to obtain additional information about interactions between the acetamide and Nb_2O_5 surface (Fig. 4A). Results showed that the C=O stretching band of acetamide adsorbed on Nb_2O_5 calcinated at 200 and 500 °C appeared at a lower wavenumber (1651 cm^{-1}) than that on Nb_2O_5 calcinated at a higher temperature (700 °C). Structural origin of the Lewis acid sites was attributed to coordinatively unsaturated superficial Nb^{5+} cations, while the structural origin of the Brønsted-acidic sites was associated predominantly with acidic superficial hydroxyl

groups as proton donors.[68] Therefore, the Nb_2O_5 calcinated at relatively low temperatures (~500 °C) had a greater number of surface defects that can serve as Lewis acid sites. In addition, these sites for the Nb_2O_5 upon calcination at low temperatures would have highly distorted Nb coordination structures that can efficiently activate the C=O bond of the amide, resulting in high activity. Surface basicity of these Nb_2O_5 catalysts were investigated by measuring O_{1s} binding energies, shown in Fig. 4B. The top peak positions of the O_{1s} binding energies decreased with increasing calcination temperature, indicating Nb_2O_5 calcined at high temperature possessed high surface basicity. These IR and XPS results indicate the presence of strong Lewis acids and relatively strong surface basicity of Nb_2O_5 prepared *via* calcination at 500 °C and reveals the best TOF among the Nb_2O_5 catalysts explored in this study.

An additional comparative study was performed to investigate the role of Lewis and Brønsted acid sites of Nb_2O_5 with other heterogenous and homogenous Brønsted acid catalysts in the hydrolysis reaction. The Na^+-exchanged Nb_2O_5 was prepared by replacing the Brønsted acid sites with Na^+ ions resulting a slightly lower number of Lewis acid sites than in Nb_2O_5 (Fig. S5). Here, Na^+-exchanged Nb_2O_5 a catalyst containing almost exclusively Lewis acidic sites, gave a rate and yield of acetic acid product similar to that of Nb_2O_5. Therefore, the hydrolysis reaction is catalyzed predominantly by the Lewis acid rather than by the Brønsted acid sites. This is supported by the poor activity of truly Brønsted acidic catalysts such as PTSA (*p*-toluenesulfonic acid) and the zeolites Hβ-20 and HMFI-20.

The influence of acetamide and water concentrations on the initial rate of formation of acetic acid also was explored, with results shown in Fig. 5. A linear relation was found for double logarithmic plots and the order (n) of the reaction was determined from the slopes of the lines with respect to acetamide and water. The acid formation rate increased with water concentration, which followed first-order reaction kinetics (n = +0.97, R^2 = 0.981), suggesting that water was involved in the kinetically important steps. Conversely, a negative slope (n = -0.20) was observed upon increasing the concentration of acetamide, which suggests that surface-adsorbed acetamide or its derivatives strongly adsorb on the Nb_2O_5 surface and inhibit the catalytic reaction.

Based on the experimental results (in-situ IR spectra of adsorbed acetamide species) and our previous computational studies on amidation of amines by carboxylic acids over Nb_2O_5,[64,76] a plausible reaction mechanism for the Nb_2O_5-catalyzed hydrolysis of acetamide to form acetic acid is proposed in Fig. 6. The catalytic cycle should start with the adsorption of acetamide on the Lewis acid sites of the Nb_2O_5 catalyst and the adsorbed acetamide activated by the nucleophilic attack of oxygen atom of water (which is pre-adsorbed by the basic surface oxygen of Nb_2O_5 catalyst) to produce acetate species. After the removal of ammonia, a negatively charged transition state of acetate and free base site of Nb_2O_5 is produced. Finally, the acetic acid would be desorbed to regenerate the free acid sites of the Nb_2O_5 catalyst.

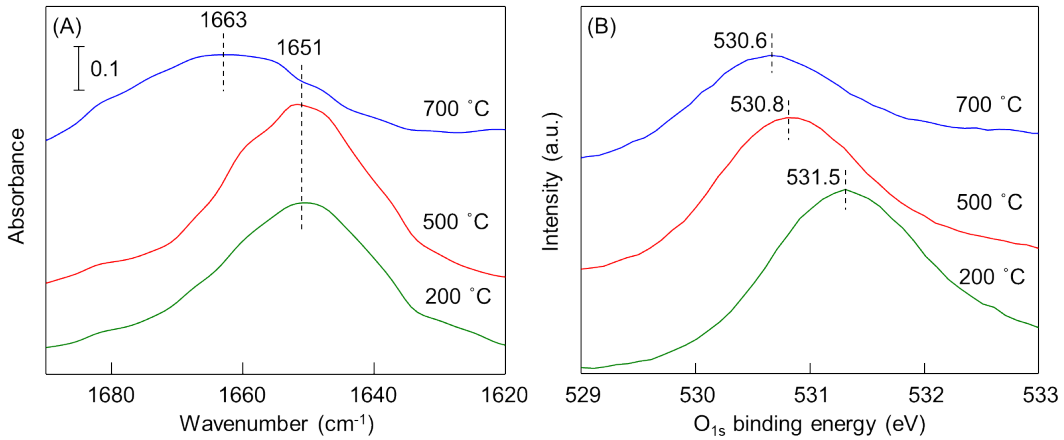

Fig. 4 (A) IR spectra of adsorbed acetamide species on Nb_2O_5 catalysts calcined at different temperatures (200, 500, and 700 °C) and (B) XPS spectra of the O_{1s} region of Nb_2O_5 catalysts calcined at different temperatures (200, 500, and 700 °C). The IR spectra were recorded at 120 °C under He flow for 200 s after introduction of acetamide (1 μL).

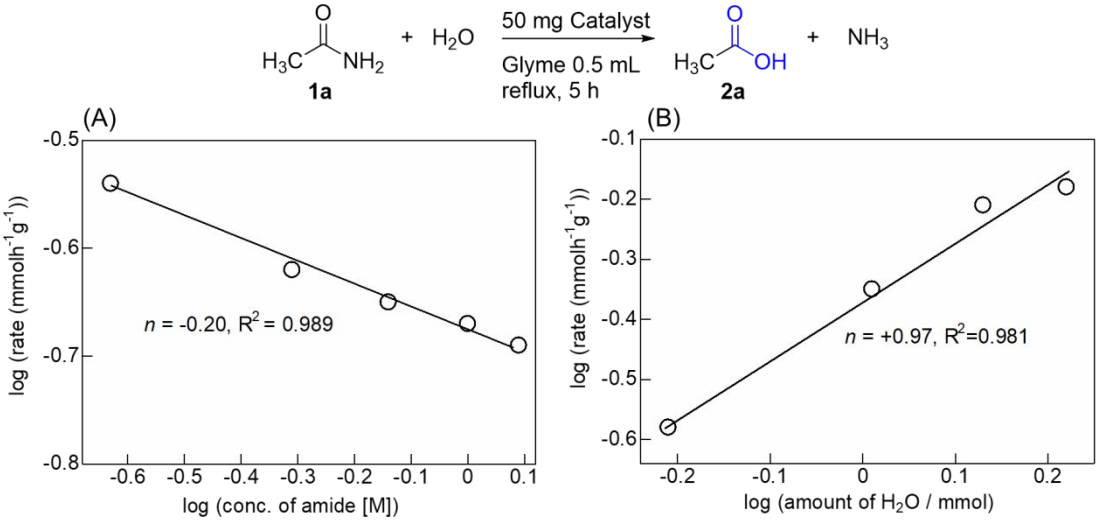

Fig. 5 Formation rate of acetic acid as a function of the concentration of (A) acetamide (0.23 M to 1.22 M) and (B) water (0.62 mmol to 1.68 mmol); reaction conditions: Nb_2O_5 (50 mg), T = 100 °C, t = 5 h.

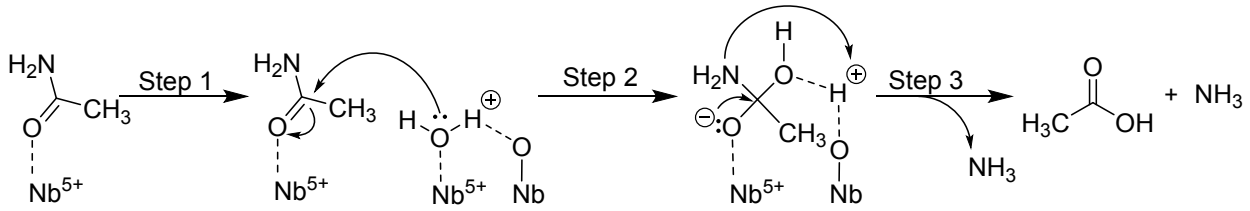

Fig. 6 Plausible reaction mechanism for the Nb_2O_5-catalyzed hydrolysis of acetamide to acetic acid.

Catalytic properties and substrate scopes

Time course of the reaction was obtained under standard reaction conditions, as shown in Figure 7A. Results of the concentration/time plot of reactive components of **1a** and **2a** revealed that the reaction time of 20 h was adequate to obtain the greatest conversion, yield, and selectivity of the product. No by-products were observed until reaction was complete. Next, a leaching test was conducted to check the heterogeneous nature of Nb_2O_5. For this purpose, after reaction for 2 h (18% yield), the solid catalyst was separated by filtration and the reaction was continued without any catalyst until 20 h. Results showed that the product yield did not increase after removal of catalyst, which confirmed that no leaching of the catalyst occurred and that the reaction stopped in the absence of the catalyst. In addition, the amount of Nb_2O_5 in the filtrate was below the detection limit as confirmed by Inductively coupled plasma-atomic emission spectroscopy (ICP-AES) analysis.

The reusability of this catalytic system was investigated using the standard reaction conditions in the conversion of **1a** to **2a** (Figure 7B). Initial reaction rate as well as the yield after each cycle were determined. No significant change in both reaction rate and yield was seen. After each cycle, the catalyst was separated from the reaction mixture by centrifugation. After separation, the catalyst was washed twice with isopropyl alcohol (2 mL) and acetone (2 mL) followed by drying at 110 °C for 5 h and then used in next cycle. The catalyst Nb_2O_5 could be reused at least 6 times, with just a slight loss in activity. However, catalytic performance could be restored easily by recalcination at 500 °C for 3 h in air.

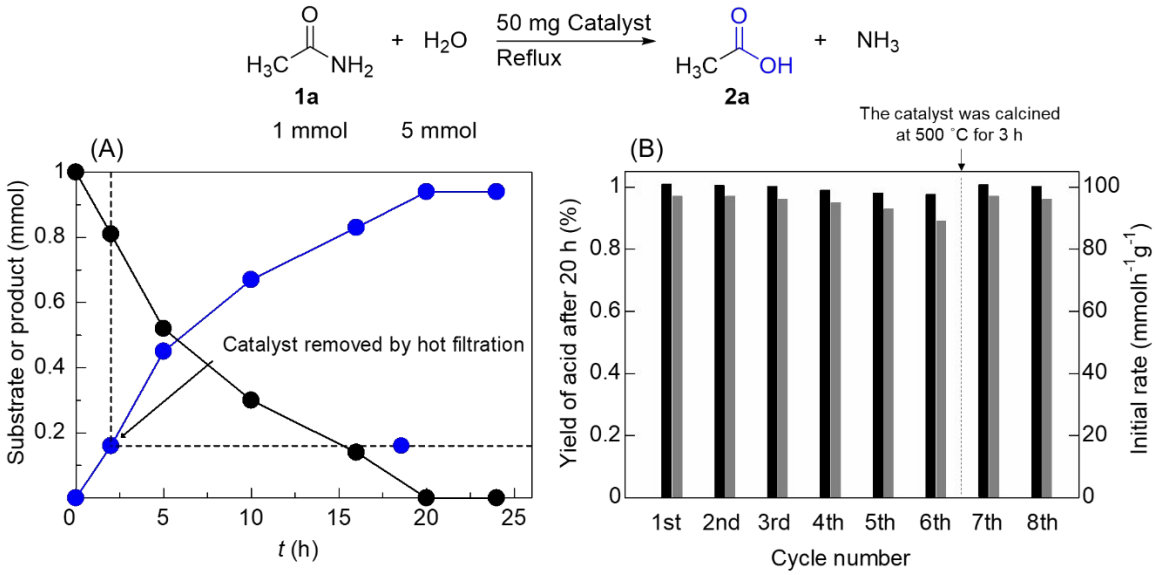

Fig. 7 (A) Time course plots for hydrolysis of acetamide **1a** to acetic acid **2a** over Nb_2O_5 catalyst calcinated at 500 °C. Acetamide (1 mmol) and water (5 mmol) were refluxed under standard reaction conditions. Reaction conditions: Nb_2O_5 (50 mg), reflux, t = 24 h (B) Catalyst reuse for hydrolysis of acetamide **1a** to acetic acid **2a** promoted by Nb_2O_5 catalyst calcinated at 500 °C under standard conditions. Black bars represent yield of **2a** after 20 h; gray bars represent initial rates of **2a** formation. After the sixth cycle, the catalyst was calcined at 500 °C for 3 h and then used in 7th and 8th cycle. Reaction conditions: reflux, t = 2 h for initial rate determination, reflux, t = 20 h for final rate determination.

After finalizing optimized reaction conditions, the applicability of the catalytic system was examined by determining the substrate scope using various amide substrates. This method was applicable for a wide range of aliphatic and aromatic amide substrates. As shown in Scheme 2**,** several aliphatic amides with different functionalities were screened. Linear amides containing short- and long-carbon chains (**1a-1e**) and benzylic (**1f, 1h**) and allylic (**1g**) amides underwent hydrolysis to their corresponding acids with excellent isolated yields (83–91%). Amides containing a cyclohexyl-substituted tertiary α-carbon (**1i**), α-stereocenter (**1j**), and sterically hindered quaternary (pivaloyl and adamantyl) amides (**1k**, **1l**) were converted to the respective acids in 83–95% isolated yield. In addition, the present catalytic system successfully transformed malonamide (**1m**) to malonic acid (**2m**, 82% isolated yield), indicating the practicability of converting two amides to two acids in the same reaction pot. Different secondary and tertiary aliphatic amides (**1n-1o**) also were tolerated and gave equivalent acids in high isolated yields (78–86%). Although this catalytic system required longer reaction times for secondary and tertiary unactivated aliphatic amides, it exhibited good performance for the *N*-MeO activated amide giving high isolated yield (88%) within 20 h.

Scheme 3 shows the hydrolysis reaction scope for different aromatic amides. A series of electron-donating (**3a-3g**) and -withdrawing (**3h-3l**) substituents containing aromatic amides were converted to their corresponding acids in good to high isolated yields (**4a-4l**, 76–87%). Sterically hindered tertiary amides, particularly *N,N*-diethyl-3-methyl-benzamide (**3c**) and *N,N*-dimethyl-3-trifluoromethyl-benzamide (**3k**), were applicable in this proposed catalytic system. Similarly, naphthyl-substituted amides (**3m**, **3n**) and N, S and O heteroatom-containing amides (**3o-3q**) also underwent hydrolysis in the present catalytic system to give good isolated yields (> 80%). In addition, two amides containing aromatic substituents, such as terephthalamide (**3r**), also were hydrolyzed into terephthalic acid (**4r**, 83%) successfully.

Applicability of the present catalytic system over different *N*-substituted secondary and tertiary aromatic amides also was investigated. Results showed that secondary and tertiary aromatic amides were transformed successfully into their corresponding carboxylic acids (**4s-4w**, 78–90% isolated yield, 36 h) where *N*-methoxy-activated amide (**3u**) was hydrolyzed more readily than other unactivated amides (**3s-3w**). Reactions of several amides (20 mmol) and water (100 mmol) on a gram scale were conducted for carboxylic acid synthesis using only 50 mg of the catalyst over 100 h. Results demonstrated that the present method was applicable for large-scale synthesis of carboxylic acids with a high turnover number (TON) as shown in Scheme 4.

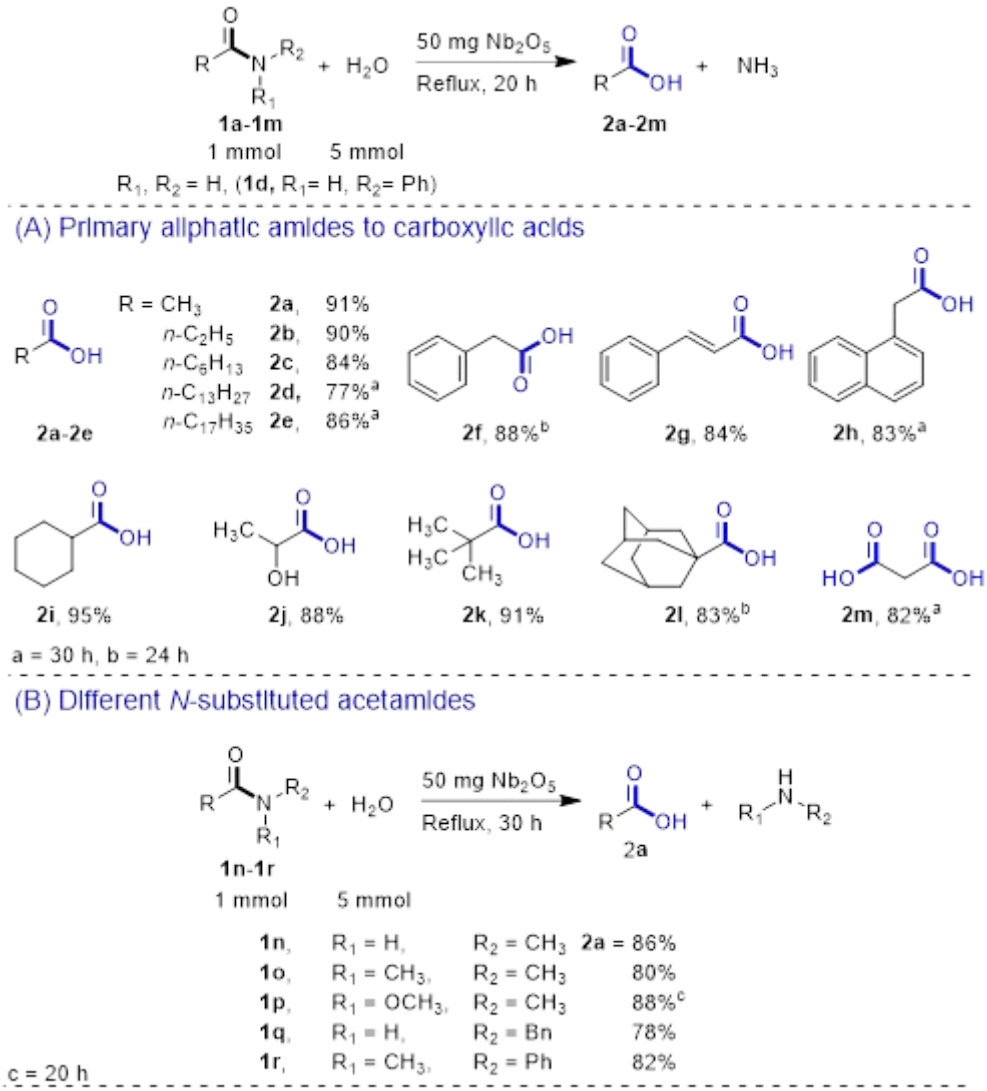

Scheme 2 Hydrolysis of different aliphatic amides to the corresponding carboxylic acids. Isolated yields are shown.

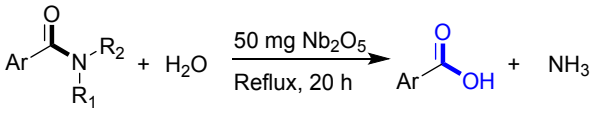

3a-3r **4a-4r**

1 mmol 5 mmol

R_1, R_2 = H, (**3c**, R_1, R_2 = Et; **3k**, R_1, R_2 = Me,)

(A) Primary aromatic amides to carboxylic acids

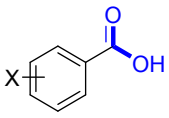

4a-4l

X = H, **4a**, 87%
= *p*-CH_3, **4b**, 80%
= *m*-CH_3, **4c**, 76%[a]
=*p*-*t*-Bu **4d**, 77%
= *p*-NH_2 **4e**, 81%
= *p*-OH **4f**, 83%
= *o*-OH **4g**, 81%
= *m*-F, **4h**, 80%[a]
= *p*-Cl, **4i**, 84%
= *p*-OCH_3, **4j**, 83%
=*m*-CF_3, **4k**, 84%[a]
= *p*-NO_2, **4l** 76%[a]

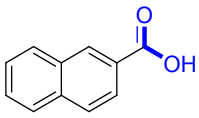

4m, 86%[b]

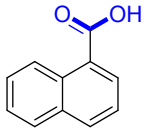

4n, 82%[b]

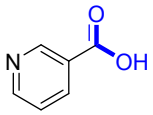

4o, 83%

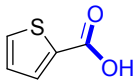

4p, 85%

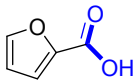

4q, 85%

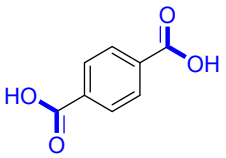

4r, 83%

a = 24 h, b = 30 h

(B) Different *N*-substituted benzamides

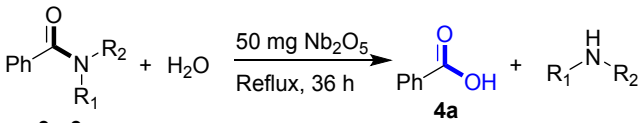

3s-3w **4a**

1 mmol 5 mmol

3s,	R_1 = H,	R_2 = CH_3	**4a** = 90%
3t,	R_1 = CH_3,	R_2 = CH_3	84%
3u,	R_1 = OCH_3,	R_2 = CH_3	82%[c]
3v,	R_1 = C_2H_5,	R_2 = C_2H_5	78%
3w,	R_1 = H,	R_2 = Ph	82%

c = 20 h

Scheme 3 Hydrolysis of different aromatic amides to the corresponding carboxylic acids. Isolated yields are shown.

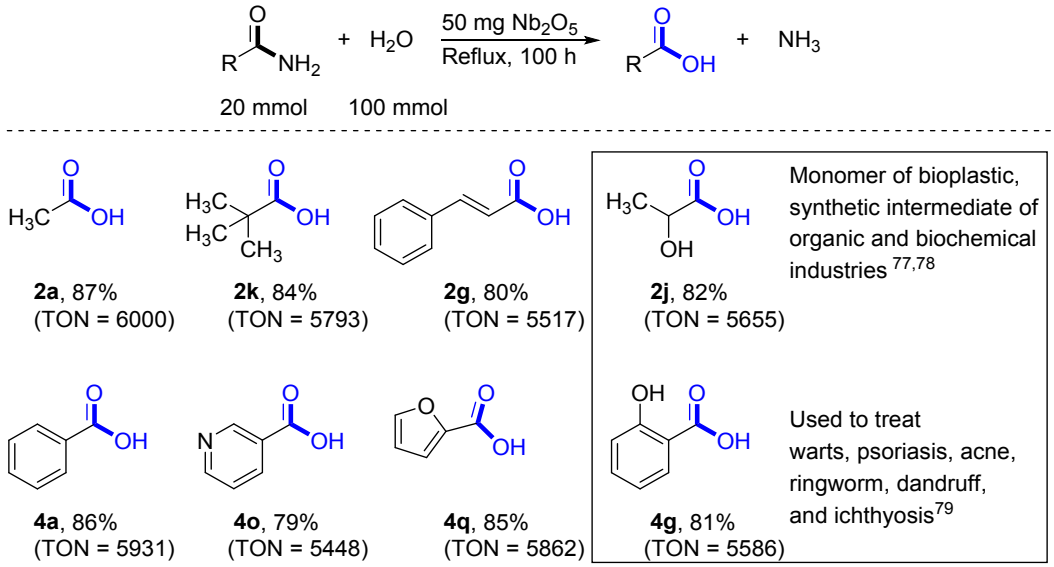

Scheme 4 Gram scale hydrolysis of amides to carboxylic acids (including lactic acid **2j** and salicylic acid **4g**).[77–79] GC yields are shown.

Conclusions

An efficient, simple, and versatile heterogenous Nb_2O_5 catalytic system has been developed for hydrolysis of amides to carboxylic acids under relatively mild conditions. The quantity and strength of Lewis acid sites of Nb_2O_5 catalysts were dependent on their structure and morphology, where surface area and number of Lewis acid sites as well as their interactions with carbonyl groups decreased with an increase in catalyst calcination temperature. Low-temperature calcined TT and/or T-phased Nb_2O_5 were more reactive in the hydrolysis than those of high-temperature calcined (M and H-phased) Nb_2O_5. The catalytic performance can be attributed mainly to the facile activation of the C=O bond of the amides by surface Nb^{5+} Lewis acid sites, which function even in the presence of basic inhibitors such as H_2O and NH_3. Moderated surface basicity also found to play a role in the efficient progression of the reaction. This heterogeneous catalytic system accepted a broad scope of amide substrates (> 40 examples; up to 95% isolated yield) with catalysts reusability, additive-free, solvent-free reaction condition and generation of ammonia and amines as byproducts from primary amides and secondary/tertiary amides respectively.

Conflicts of interest

There are no conflicts to declare

Acknowledgements

This study was supported financially by JSPS KAKENHI grants 17H01341, 19K05556, 20K05576, 20H02775, and 20H02518 from the Japan Society for the Promotion of Science (JSPS) and by the Japanese Ministry of Education, Culture, Sports, Science, and Technology (MEXT) within the projects "Integrated Research Consortium on Chemical Sciences (IRCCS)" and "Elements Strategy Initiative to Form Core Research Center", as well as by the JST-CREST project JPMJCR17J3. The authors are indebted to the technical division of the Institute for Catalysis (Hokkaido University) for manufacturing experimental equipment.

Notes and references

1 N. E. Wezynfeld, T. Frączyk and W. Bal, *Coord. Chem. Rev.*, 2016, **327**–**328**, 166–187.

2 Y. Kita, Y. Nishii, T. Higuchi and K. Mashima, *Angew. Chemie Int. Ed.*, 2012, **51**, 5723–5726.

3 L. Hie, N. F. Fine Nathel, T. K. Shah, E. L. Baker, X. Hong, Y.-F. Yang, P. Liu, K. N. Houk and N. K. Garg, *Nature*, 2015, **524**, 79–83.

4 P. Lei, G. Meng and M. Szostak, *ACS Catal.*, 2017, 1960–1965.

5 T. Deguchi, H. L. Xin, H. Morimoto and T. Ohshima, *ACS Catal.*, 2017, **7**, 3157–3161.

6 A. A. Kadam, T. L. Metz, Y. Qian and L. M. Stanley, *ACS Catal.*, 2019, **9**, 5651−5656.

7 H. Nagae, T. Hirai, D. Kato, S. Soma, S. Akebi and K. Mashima, *Chem. Sci.*, 2019, **10**, 2860–2868.

8 M. N. Rashed, S. M. A. H. Siddiki, A. S. Touchy, M. A. R. Jamil, S. S. Poly, T. Toyao, Z. Maeno and K. Shimizu, *Chem. – A Eur. J.*, 2019, **25**, 10594–10605.

9 T. Toyao, M. Nurnobi Rashed, Y. Morita, T. Kamachi, S. M. A. Hakim Siddiki, M. A. Ali, A. S. Touchy, K. Kon, Z. Maeno, K. Yoshizawa and K. ichi Shimizu, *ChemCatChem*, 2019, **11**, 449–456.

10 N. V Kaminskaia and N. M. Kostić, *Inorg. Chem.*, 1998, **37**, 4302–4312.

11 G. Li, P. Lei and M. Szostak, *Org. Lett.*, 2018, **20**, 5622–5625.

12 J. E. Dander and N. K. Garg, *ACS Catal.*, 2017, 1413–1423.

13 K. Mashima, Y. Nishii and H. Nagae, *Chem. Rec.*, 2020, **20**, 332–343.

14 A. Shrotri, H. Kobayashi and A. Fukuoka, *Acc. Chem. Res.*, 2018, **51**, 761–768.

15 V. Gotor, V. Gotor-Fernández and E. Busto, *Compr. Chirality*, 2012, **7**, 101–121.

16 Y. Izumi, *Catal. Today*, 1997, **33**, 371–409.

17 S. Mahesh, K. C. Tang and M. Raj, *Molecules*, , DOI:10.3390/molecules23102615.

18 H. G. T. Ly, G. Absillis, R. Janssens, P. Proost and T. N. Parac-Vogt, *Angew. Chemie - Int. Ed.*, 2015, **54**, 7391–7394.

19 G. Absillis and T. N. Parac-Vogt, *Inorg. Chem.*, 2012, **51**, 9902–9910.

20 A. Sap, G. Absillis and T. N. Parac-Vogt, *Dalt. Trans.*, 2015, **44**, 1539–1548.

21 K. Stroobants, E. Moelants, H. G. T. Ly, P. Proost, K. Bartik and T. N. Parac-Vogt, *Chem. - A Eur. J.*, 2013, **19**, 2848–2858.

22 T. Takarada, M. Yashiro and M. Komiyama, *Chem. - A Eur. J.*, 2000, **6**, 3906–3913.

23 J. Ni, Y. Sohma and M. Kanai, *Chem. Commun.*, 2017, **53**, 3311–3314.

24 H. G. T. Ly, G. Fu, A. Kondinski, B. Bueken, D. De Vos and T. N. Parac-Vogt, *J. Am. Chem. Soc.*, 2018, **140**, 6325–6335.

25 C. O'Connor, *Q. Rev. Chem. Soc.*, 1970, **24**, 553–564.

26 R. J. Ouellette and J. D. Rawn, *Org. Chem.*, 2014, 659–698.

27 M. L. Bender, *Chem. Rev.*, 1960, **60**, 53–113.

28 L. Meriwether and F. H. Wbstheimer, *J. Am. Chem. Soc.*, 1956, **78**, 5119–5123.

29 A. M. Barrios and S. J. Lippard, *J. Am. Chem. Soc.*, 1999, **121**, 11751–11757.

30 M. M. Heravi, D. Zargarani and S. Khaleghi, *J. Chem. Res.*, 2005, **2005**, 119–120.

31 X. Zhang, K. Luo, W. Chen and L. Wang, *Chinese J. Chem.*, 2011, **29**, 2209–2212.

32 S. M. A. H. Siddiki, M. N. Rashed, M. A. Ali, T. Toyao, P. Hirunsit, M. Ehara and K. Shimizu, *ChemCatChem*, 2019, **11**, 383–396.

33 M. Tamura, K. Shimizu and A. Satsuma, *Chem. Lett.*, 2012, **41**, 1397–1405.

34 S. M. A. H. Siddiki, A. S. Touchy, M. Tamura and K. Shimizu, *RSC Adv.*, 2014, **4**, 35803–35807.

35 T. Kamachi, S. M. A. H. Siddiki, Y. Morita, M. N. Rashed, K. Kon, T. Toyao, K. Shimizu and K. Yoshizawa, *Catal. Today*, 2018, **303**, 256–262.

36 A. Corma and H. García, *Chem. Rev.*, 2003, **103**, 4307–4365.

37 H. Yamamoto, Ed., *Lewis Acids in Organic Synthesis*, Wiley, 2000.

38 D. Schinzer, Ed., *Selectivities in Lewis Acid Promoted Reactions*, Springer Netherlands, Dordrecht, 1989.

39 S. Kobayashi and K. Manabe, *Acc. Chem. Res.*, 2002, **35**, 209–217.

40 Y. Koito, K. Nakajima, H. Kobayashi, R. Hasegawa, M. Kitano and M. Hara, *Chem. - A Eur. J.*, 2014, **20**, 8068–8075.

41 S. Kobayashi and I. Hachiya, *J. Org. Chem.*, 1994, **59**, 3590–3596.

42 S. Kobayashi and C. Ogawa, *Chem. - A Eur. J.*, 2006, **12**, 5954–5960.

43 S. Kobayashi, *European J. Org. Chem.*, 1999, 15–27.

44 P. Hirunsit, T. Toyao, S. M. A. H. Siddiki, K. Shimizu and M. Ehara, *ChemPhysChem*, 2018, **19**, 2848–2857.

45 Q. Sun, Y. Fu, H. Yang, A. Auroux and J. Shen, *J. Mol. Catal. A Chem.*, 2007, **275**, 183–193.

46 K. Nakajima, T. Fukui, H. Kato, M. Kitano, J. N. Kondo, S. Hayashi and M. Hara, *Chem. Mater.*, 2010, **22**, 3332–3339.

47 H. T. Kreissl, K. Nakagawa, Y. K. Peng, Y. Koito, J. Zheng and S. C. E. Tsang, *J. Catal.*, 2016, **338**, 329–339.

48 A. J. M. Van Dijk, R. Duchateau, E. J. M. Hensen, J. Meuldijk and C. E. Koning, *Chem. - A Eur. J.*, 2007, **13**, 7673–7681.

49 G. S. Foo, D. Wei, D. S. Sholl and C. Sievers, *ACS Catal.*, 2014, **4**, 3180–3192.

50 S. Furukawa, Y. Ohno, T. Shishido, K. Teramura and T. Tanaka, *ACS Catal.*, 2011, **1**, 1150–1153.

51 S. Furukawa, T. Shishido, K. Teramura and T. Tanaka, *ChemPhysChem*, 2014, **15**, 2665–2667.

52 A. Takagaki, D. Lu, J. N. Kondo, M. Hara, S. Hayashi and K. Domen, *Chem. Mater.*, 2005, **17**, 2487–2489.

53 K. Yamashita, M. Hirano, K. Okumura and M. Niwa, *Catal. Today*, 2006, **118**, 385–391.

54 K. Nakajima, Y. Baba, R. Noma, M. Kitano, J. N. Kondo, S. Hayashi and M. Hara, *J. Am. Chem. Soc.*, 2011, **133**, 4224–4227.

55 K. Skrodczky, M. M. Antunes, X. Han, S. Santangelo, G. Scholz, A. A. Valente, N. Pinna and P. A. Russo, *Commun. Chem.*, 2019, **2**, 129.

56 T. Fuchigami, M. Kuroda, S. Nakamura, M. Haneda and K. I. Kakimoto, *Nanotechnology*, 2020, **31**, 325705.

57 T. Murayama, J. Chen, J. Hirata, K. Matsumoto and W. Ueda, *Catal. Sci. Technol.*, 2014, **4**, 4250–4257.

58 G. S. Nair, E. Adrijanto, A. Alsalme, I. V. Kozhevnikov, D. J. Cooke, D. R. Brown and N. R. Shiju, *Catal. Sci. Technol.*, 2012, **2**, 1173–1179.

59 M. N. Rashed, S. M. A. H. Siddiki, M. A. Ali, S. K. Moromi, A. S. Touchy, K. Kon, T. Toyao and K. Shimizu, *Green Chem.*, 2017, **19**, 3238–3242.

60 M. A. Ali, S. M. A. H. Siddiki, K. Kon, J. Hasegawa and K. Shimizu, *Chem. - A Eur. J.*, 2014, **20**, 14256–14260.

61 M. A. Ali, S. M. A. H. Siddiki, W. Onodera, K. Kon and K. Shimizu, *ChemCatChem*, 2015, **7**, 3555–3561.

62 M. A. Ali, S. M. A. H. Siddiki, K. Kon and K. Shimizu, *ChemCatChem*, 2015, **7**, 2705–2710.

63 M. A. Ali, S. K. Moromi, A. S. Touchy and K. I. Shimizu, *ChemCatChem*, 2016, **8**, 891–894.

64 P. Hirunsit, T. Toyao, S. M. A. H. Siddiki, K. Shimizu and M. Ehara, *ChemPhysChem*, 2018, **19**, 2848–2857.

65 K. Nakajima, Y. Baba, R. Noma, M. Kitano, J. N. Kondo, S. Hayashi and M. Hara, *J. Am. Chem. Soc.*, 2011, **133**, 4224–4227.

66 M. B. Pinto, A. L. Soares, A. Mella Orellana, H. A. Duarte and H. A. De Abreu, *J. Phys. Chem. A*, 2017, **121**, 2399–2409.

67 K. Tamai, K. Murakami, S. Hosokawa, H. Asakura, K. Teramura and T. Tanaka, *J. Phys. Chem. C*, 2017, **121**, 22854–22861.

68 H. T. Kreissl, M. M. J. Li, Y. K. Peng, K. Nakagawa, T. J. N. Hooper, J. V. Hanna, A. Shepherd, T. S. Wu, Y. L. Soo and S. C. E. Tsang, *J. Am. Chem. Soc.*, 2017, **139**, 12670–12680.

69 Y. Nagai, T. Hirabayashi, K. Dohmae, N. Takagi, T. Minami, H. Shinjoh and S. Matsumoto, *J. Catal.*, 2006, **242**, 103–109.

70 K. Shimizu, W. Onodera, A. S. Touchy, S. M. A. H. Siddiki, T. Toyao and K. Kon, *ChemistrySelect*, 2016, **1**, 736–740.

71 C. Chaudhari, S. M. A. Hakim Siddiki, M. Tamura and K. Shimizu, *RSC Adv.*, 2014, **4**, 53374–53379.

72 R. A. Rani, A. S. Zoolfakar, A. P. O'Mullane, M. W. Austin and K. Kalantar-Zadeh, *J. Mater. Chem. A*, 2014, **2**, 15683–15703.

73 E. I. Ko and J. G. Weissman, *Catal. Today*, 1990, **8**, 27–36.

74 R. Kodama, Y. Terada, I. Nakai, S. Komaba and N. Kumagai, *J. Electrochem. Soc.*, 2006, **153**, A583.

75 M. Tamura, K. Shimizu and A. Satsuma, *"Applied Catal. A, Gen.*, 2012, **433**–**434**, 135–145.

76 M. B. Pinto, A. L. Soares, M. C. Quintão, H. A. Duarte and H. A. De Abreu, *J. Phys. Chem. C*, 2018, **122**, 6618–6628.

77 K. J. Jem and B. Tan, *Adv. Ind. Eng. Polym. Res.*, 2020, **3**, 60–70.

78 C. Rodrigues, L. P. S. Vandenberghe, A. L. Woiciechowski, J. de Oliveira, L. A. J. Letti and C. R. Soccol, *Curr. Dev. Biotechnol. Bioeng. Prod. Isol. Purif. Ind. Prod.*, 2016, 543–556.

79 P. E. Grimes, *Dermatologic Surg.*, 1999, **25**, 18–22.

1
2
3